ОБЪЕДИНЕННЫЙ
ИНСТИТУТ
ЯДЕРНЫХ
ИССЛЕДОВАНИЙ

Дубна

E4-98-121

Ş.Mişicu*

TRAJECTORY CALCULATIONS FOR THE TERNARY COLD FISSION OF ^{252}Cf

Submitted to «Ядерная физика»

*Department for Theoretical Physics, National Institute for Nuclear Physics, Bucharest-Măgurele, Romania

1998

I. INTRODUCTION

The cold ternary fission is a rearrangement process of a large group of nucleons from the ground state of the initial nucleus to the ground state of the three final fragments. Like in the case of spontaneous and thermal-induced fission a ternary component of a few tenths of percent is present also in the cold fission process [1–3].

In order to determine the configuration and the dynamics of the fissioning nucleus at scission, the experimental data for the light charged particle (LCP) emitted in the fragmentation process are analyzed and compared with the theoretical results obtained via trajectory calculations. In the past a large number of studies were devoted to the trajectory calculation, specially for α-particles in the point charge approximation and without the account of nuclear forces. The alphas were considered to be emitted from the neck region [4–9]. There have been also some authors who considered the finite size and the deformation effects [10–12] and showed that these geometrical factors are influencing sensitively the angular distributions of the LCP.

However in all these approaches to the ternary spontaneous fission the problem of choosing the initial parameters of the trajectory calculations is complicated by the fact that various theories give different predictions. Since only the energies and the angles of the three particles can be experimentally determined, solving the equations of motion backward in time will not provide a full information on the geometric and dynamic characteristics of the fissioning system at the moment of the LCP-emission. The only possibility is to probe various combinations of assumed initial conditions and then compute the trajectories for comparison with the available experimental data. In the *hot* ternary fission the initial conditions are so numerous that in order to encompass as much as possible combinations, Monte-Carlo techniques were

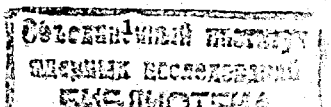

employed [11,12].

For the cold ternary fission the initial conditions are better known [3,14]. First of all the fragment deformations are those of their ground states. This fact prompted us to calculate the final characteristics of the LCP emitted in the cold fission of ^{252}Cf for different mass splittings, and see how the static deformations and the finite size are modifying the outcome of the trajectory calculation. Using forces, computed through a double folded integration of the Coulomb interaction between two quadrupole deformed heavy ions, we derived the equations of motion for the three-body problem, and solved them numerically . The solution of this set of equations provided the final angle of the LCP with respect to the fission axis and its kinetic energy. We compared our calculations with the point-like trajectory and some experimental consequences were discussed.

II. DETERMINATION OF THE INITIAL CONDITIONS

Usually, in trajectory calculations for the spontaneous fission different choices are taken for the initial kinetic energies of the fragments emitted in the process. For example the initial kinetic energy of the two main fragments and of the α emitted in the spontaneous ternary fission should be around 0.5 MeV according to the statistical theory and the equipartition principle [7,8]. On the contrary, in the dynamical theory of fission [13] the nascent fragments at scission are predicted to be moving with appreciable kinetic energy (20-50 MeV). The initial velocities of the heavy fragments are considered to have non-zero components only along the x-axis. The initial velocity of the light fragment $v_L(0)$ is related to the initial velocity of the heavy fragment $v_H(0)$ in such a way that the total momentum of the two fission fragments is zero along the x-axis, i.e. $v_L(0) = \frac{A_H}{A_L} v_H(0)$. This reasonable

assumption will be applied by us also.

Therefore we have to determine the following initial conditions : a) The tip distance d; b) the kinetic energies of the two main fragments E_{H0}, E_{L0} and the kinetic energy of the LCP E_{LCP}; c) the initial geometric configuration of the LCP, i.e. the position between the fragments and the angle θ^0_{LCP} between the direction of motion of the LCP and the axis joining the two main fragments; d) The shape of the fragments.

The determination of these quantities in the ternary cold fission will be facilitated, up to a certain extent, by the peculiar characteristic of the process, i.e. the fragments are emitted with total kinetic energy TKE close to the corresponding ternary decay energy Q_t. In order to achieve such large TKE values, the three final fragments should have very compact shapes at the scission point and deformations close to those of their ground states, similar to the case of the cold binary fragmentations. One may next suppose that the shapes of the fragments will not be modified when the fragments move away in the Coulomb field of each other. Thus, the problem of the fragments shape in the initial configuration is easily established for the cold fission.

In order to determine the kinetic energies of the two main fragments we make use of the considerations derived from the deformed cluster model that we employed in previous papers for the study of the ternary cold fission [14]. In this deformed cluster model the barrier between heavy fragments (for binary fission) and the barrier between the LCP and the heavier fragments (for ternary fission) can be calculated quite accurately due to the fact that the touching configurations are situated inside of the barriers. For the two fragments, the exit point from the potential barrier is at a tip distance d around 3 fm, as can be seen in Figure 1, for the case ^{248}Cm $\rightarrow$ ^{104}Mo + ^{144}Xe. This barrier is much thinner than the barrier between the LCP and the

heavier fragments, and thus in our model first the two heavier fragments penetrate the potential barrier between them and later on the LCP is emitted. Consequently the mass distributions of the heavier fragments are very similar to those of the cold binary fission of an initial nucleus leading to the same heavy fragments, i.e. ^{248}Cm if the LCP is an α [15], or ^{242}Pu if the LCP is ^{10}Be [14]. The decay energy for such a binary fragmentation will be $Q_{LH} = Q_t - Q_{LCP}$, where Q_t is the ternary decay energy of ^{252}Cf and Q_{LCP} is 6.22 MeV for α and 8.71 MeV for ^{10}Be.

On ground of the cold fission characteristics mentioned above one may conjecture that at the exit point (second turning point) of the two heavier fragments, their potential energy is equal to Q_{LH} and their kinetic energy is equal to zero. When the fragments move apart, i.e. their tip distance increases, their kinetic energy increases too. In order to estimate the total kinetic energy of the fragments we have to find out at which tip distance the release of the LCP is likely to occur and compute at that point the potential energy, i.e.

$$TKE(d) \equiv TKE_L + TKE_H = Q_{LH} - V_{LH}(d) \qquad (1)$$

Using the conservation of linear momentum invoked above we have

$$TKE_L = \frac{A_H}{A_L} TKE_H \qquad (2)$$

and the individual kinetic energies in terms of the total kinetic energy read

$$TKE_i = \frac{A_i}{A_H + A_L} TKE(d) \quad (i = L, H)\,. \qquad (3)$$

Now we turn to the problem of determining the tip distance d. It is reasonable to suppose that d should correspond to the configuration at which the LCP is released. In Figures 2a and 2b we plotted the ternary potential seen by the LCP (in this case an α) in the field of the two heavy fragments. As we shall see later the LCP should stay between the two heavy fragments in a position which should avoid its absorbtion

by any of the fragments. We see in Figure 2a, that for tip distances up to 7 fm, the α is facing a thick barrier in the transversal direction. Eventually as the distance between the fragments increases the pocket in which the α is located becomes more and more shallower untill it disapears around $d = 8$ fm. Therefore one may conclude from these qualitative arguments that the initial tip distance between the two main fragments should not be larger than that corresponding to the disappearence of the LCP pocket. On the other hand for tip distances smaller than 6 fm the emission of the α is strongly hindered by a thick barrier even for a rather high zero energy $E^0_\alpha \geq 3$MeV (see Fig.3).

If we choose $d = 8$ fm for the example considered in Figure 1, then we get for the total kinetic energy of the two main fragments TKE=46.21 MeV which is much larger than the corresponding kinetic energy in the spontaneous fission. For $d = 6$ fm the kinetic energy will drop to TKE=28.78 MeV. Repeating this calculation for other mass splittings we conclude that the kinetic energy of the main fragments is ranging in the broad interval 25 - 50 MeV, but as we shall see bellow it is correlated to the kinetic energy of the emitted alfa particle through the tip distance.

We are left now with the determination of the LCP geometrical and dynamical initial characteristics. For that we invoke a receipt proposed by Boneh et al. [5] which consider as a possible choice for the LCP position, the point of minimum potential energy (the saddle point of the potential energy surface). If the heavy-fragments would have to interact with the LCP via point-like Coulomb forces, this electrostatic saddle point would be determined by $Z_H/R^2_{\alpha H} = Z_L/R^2_{\alpha L}$, where $R_{\alpha i}(i = L, H)$ is the distance between the LCP and the main fragment i. It is readily seen from Figure 2a,b that in the case of our deformation dependent cluster model, where the nuclear forces are introduced via the M3Y potential, this saddle point corresponds to the position where the combined Coulomb and nuclear forces exerted by the heavy

fragments on the LCP cancel each other and the potential surface will have a relative minima at this point. To establish more precisely the location of this *electro-nuclear* saddle point, we use the multipolar decomposition for the M3Y potential [16], and the above condition translates to

$$\sum_{\lambda} \frac{\partial V^{000}_{\lambda 0 \lambda}(R_{\alpha H})}{\partial R_{\alpha H}} = \sum_{\lambda} \frac{\partial V^{000}_{\lambda 0 \lambda}(R_{\alpha L})}{\partial R_{\alpha L}} \tag{4}$$

which is a generalization of the point-like Coulomb equilibrum condition. In the laboratory frame of reference, we choose the z-axis as the initial fissioning axis of the two heavier fragments, with the origin at the tip of the left (heavy) fragment. Then the location of the electrostatic saddle point is given analitically by the formula

$$z_{\alpha}(d) = \frac{d + a_L + a_H}{1 + \sqrt{Z_L/Z_H}} - a_L \tag{5}$$

where a_i $(i = L, H)$ are the major axes of the quadrupole deformed main fragments. For the pair considered in Fig.1-3, $z_{\alpha}(d) \approx 0.58d$ using the point-like Coulomb forces and $0.51d$ in our model where nuclear forces are included too.

As we already noted above the potential energy of the LCP positioned at the electro-nuclear saddle point will have a minimum in the y-direction. It is clear that the LCP can have no component of its velocity along the x-axis since this would result in a possible absorbtion of the LCP by the deep potential wells of the two heavier fragments instead of being emitted [1]. The only possibility for the LCP to *survive* the descent of the decaying system from scission to the release point is to have a momenta directed only along the y-axis. As can be inferred from Figure 2 the locus of the saddle point is on the bottom of the potential well. Taking

[1] In the case we would employ forces with repulsive nuclear core the LCP will be once again prevented to move in the z-direction.

sections of the potential surface along the y-axis at z corresponding to the saddle point, the resulting potential slice will look similar to a one-dimensional harmonic potential well (see Figure 3). When the tip distance increases, the well becomes more and more shallower untill it vanishes completely. Following an idea from [11] we will approximate the potential V_{LCP} with an harmonic potential in the y-direction, centered at the saddle-point

$$V_{LCP} \approx V_{saddle} + \frac{1}{2} C y^2 \tag{6}$$

where $V_{saddle} = V_{LCP}(z = z_{saddle}, y = 0)$ and $C = \frac{\partial^2 V_{LCP}}{\partial y^2}\Big|_{y=0}$ is the stifness. It can be shown after some algebra that the elastic constant value is given by the expression

$$C = \sum_{i=L,H} \frac{1}{R^0_{\alpha i}} \sum_{\lambda \geq 0} \left(\frac{\partial V_{\lambda 0 \lambda}(R_{\alpha i})}{\partial R_{\alpha i}}\Big|_0 - \frac{\lambda(\lambda+1)}{2} \frac{V_{\lambda 0 \lambda}(R_{\alpha i})}{R_{\alpha i}} \right) \tag{7}$$

where $R_{\alpha i}$ is the distance from the fragment i to the LCP (α) on the z-axis :

$$R^0_{\alpha L} = \frac{D}{1 + \sqrt{\frac{Z_L}{Z_H}}}, R^0_{\alpha H} = \frac{D}{1 + \sqrt{\frac{Z_H}{Z_L}}}; \tag{8}$$

where D is the inter-fragment distance. From here we get an estimation for the initial kinetic energy of the LCP supposing that it can be identified with the zero-energy in the *harmonic* potential well, i.e.

$$E_{LCP} = \frac{1}{2} \hbar \sqrt{\frac{C}{m_{LCP}}}. \tag{9}$$

Consequently, a degree of uncertainty in the initial kinetic energy occurs also for the LCP. For increasing tip distance the kinetic energy of the LCP decreases. One might suppose that in the range 6 - 8 fm, for the tip distance, the LCP has the possibility to escape by tunneling or by the disappearence of the barrier. Further the velocity corresponding to this kinetic energy, $v_{\alpha} = \sqrt{\frac{2E_{LCP}}{m_{LCP}}}$ will have a nonzero component only with respect to the y-axis, according to the above discussion.

III. TRAJECTORY EQUATIONS

In order to write down the equations of motion we have to establish the geometry of the system not only at the beginning but also long after the release of the LCP. The forces being central, and the initial velocities are in-plane the problem is simplified by a two-dimensional approximation. There will be required six coordinates and six velocities, which are governed by a system of twelve first order ordinary differential equations. In Fig. 4, we see the three fragments and the forces acting between them, just after the release of the LCP. Contrary to other works we take into account the forces exerted by the LCP on the fragments. After deriving the initial conditions in the previous section, taking into account the nuclear forces in the calculation of the barriers, we proceed now to the calculation of the trajectories by considering only the Coulomb forces. Since the kinetic energies of the fragments are rather high, this approximation is good even in the point-charge approximation.

In previous papers [3,14,17] we used a double folding potential for the heavy-ion interaction. Presently we shall consider only the Coulomb part of this interaction, between two ions, i.e.

$$V_C(\boldsymbol{R}) = \int d\boldsymbol{r}_1 \int d\boldsymbol{r}_2 \frac{\rho_1(\boldsymbol{r}_1)\rho_2(\boldsymbol{r}_2)}{|\boldsymbol{r}_1 + \boldsymbol{R} - \boldsymbol{r}_2|} \tag{10}$$

where $\rho_{1(2)}(\boldsymbol{r})$ are the charge ground-state one-body densities of the fragments. The one-body densities are taken as Fermi distributions in the intrinsic frame for axial-symmetric nuclei

$$\rho(\boldsymbol{r}) = \frac{\rho_0}{1 + e^{\frac{r - R(\theta)}{a}}} \tag{11}$$

with $R(\theta) = R_0(1 + \sum_{\lambda \geq 2} \beta_\lambda Y_{\lambda 0}(\theta, 0))$. In what follows we consider that the symmetry axes of the fragments are lying in the same plane. Using the formalism

presented in [16], the interaction between two heavy ions with orientation ω_1, ω_2 of their intrinsic symmetry axes with respect to the fixed frame, reads:

$$V(\boldsymbol{R}_{12}) = \sum_{\lambda_1,\lambda_2,\lambda_3,\mu} V^{\mu -\mu 0}_{\lambda_1\lambda_2\lambda_3}(R_{12}) P^{\mu}_{\lambda_1}(\cos\omega_1) P^{-\mu}_{\lambda_2}(\cos\omega_2) P_{\lambda_3}(\cos\Omega_{12}) \tag{12}$$

where

$$V^{\mu -\mu 0}_{\lambda_1\lambda_2\lambda_3}(R_{12}) = \frac{2}{\pi} i^{\lambda_1 - \lambda_2 - \lambda_3} \hat{\lambda}_1 \hat{\lambda}_2 C^{\lambda_1\lambda_2\lambda_3}_{0\,0\,0} C^{\lambda_1\lambda_2\lambda_3}_{\mu -\mu\, 0} F_{\lambda_1\lambda_2\lambda_3}(R_{12}) \tag{13}$$

with $P^{\mu}_{\lambda_1}(\cos\omega_1)$ and $P^{-\mu}_{\lambda_2}(\cos\omega_2)$ being the associated Legendre polynomials which describe the relative orientation of the two fragments whereas $P_{\lambda_3}(\cos\Omega_{12})$ describes the orientation of the axis joining the two nuclei with respect to the laboratory frame. In the present study the LCP is spherical and thus the interaction between the LCP and one heavy fragment $i(=L, H)$ will get a simplified form

$$V(\boldsymbol{R}_{ci}) = \sum_{\lambda} V^{000}_{\lambda 0 \lambda}(R_{ci}) P_\lambda(\cos\theta_i)\,. \tag{14}$$

The following approximation can be applied for the two heavy fragments : Since their relative orientation does not change significantly at the beginning of the quasiclassical motion, one can neglect the relative orientation of the heavy fragments:

$$V(\boldsymbol{R}_{LH}) = \sum_{\lambda_1\lambda_2\lambda_3} V^{0\,0\,0}_{\lambda_1\lambda_2\lambda_3}(R_{LH}) P_{\lambda_3}(\cos\theta_{LH})\,. \tag{15}$$

The force acting between a pair of fragments can be written:

$$\boldsymbol{F}_{ij} = -\boldsymbol{\nabla} V(\boldsymbol{R}_{ij})\,. \tag{16}$$

The force acting between the two heavy fragments is given by:

$$\begin{aligned} \boldsymbol{F}_{LH} = & -\boldsymbol{e}_x \sum_{\lambda_1\lambda_2\lambda_3} \left(\frac{\partial V^{0\,0\,0}_{\lambda_1\lambda_2\lambda_3}(R_{LH})}{\partial R_{LH}} P_{\lambda_3}(\cos\phi)\cos\phi - \frac{V^{0\,0\,0}_{\lambda_1\lambda_2\lambda_3}(R_{LH})}{R_{LH}} P^1_{\lambda_3}(\cos\phi)\sin\phi \right) \\ & - \boldsymbol{e}_y \sum_{\lambda_1\lambda_2\lambda_3} \left(\frac{\partial V^{0\,0\,0}_{\lambda_1\lambda_2\lambda_3}(R_{LH})}{\partial R_{LH}} P_{\lambda_3}(\cos\phi)\sin\phi + \frac{V^{0\,0\,0}_{\lambda_1\lambda_2\lambda_3}(R_{LH})}{R_{LH}} P^1_{\lambda_3}(\cos\phi)\cos\phi \right) \end{aligned} \tag{17}$$

whereas the forces exerted by the fragments on the LCP read:

$$F_{H\alpha}= -e_x \left(\sum_{\lambda\geq 0} \frac{\partial V^{\,0\,0\,0}_{\lambda\,0\,\lambda}(R_{\alpha H})}{\partial R_{\alpha H}} P_\lambda(\cos\psi_1)\cos\psi_1 - \sum_{\lambda\geq 2} \frac{V^{\,0\,0\,0}_{\lambda\,0\,\lambda}(R_{\alpha H})}{R_{\alpha H}} P^1_\lambda(\cos\psi_1)\sin\psi_1 \right)$$

$$- \; e_y \left(\sum_{\lambda\geq 0} \frac{\partial V^{\,0\,0\,0}_{\lambda\,0\,\lambda}(R_{\alpha H})}{\partial R_{\alpha H}} P_\lambda(\cos\psi_1)\sin\psi_1 + \sum_{\lambda\geq 2} \frac{V^{\,0\,0\,0}_{\lambda\,0\,\lambda}(R_{\alpha H})}{R_{\alpha H}} P^1_\lambda(\cos\psi_1)\cos\psi_1 \right) \quad (18)$$

$$F_{L\alpha}= e_x \left(\sum_{\lambda\geq 0} \frac{\partial V^{\,0\,0\,0}_{\lambda\,0\,\lambda}(R_{\alpha L})}{\partial R_{\alpha L}} P_\lambda(\cos\psi_2)\cos\psi_2 - \sum_{\lambda\geq 2} \frac{V^{\,0\,0\,0}_{\lambda\,0\,\lambda}(R_{\alpha L})}{R_{\alpha L}} P^1_\lambda(\cos\psi_2)\sin\psi_2 \right)$$

$$- \; e_y \left(\sum_{\lambda\geq 0} \frac{\partial V^{\,0\,0\,0}_{\lambda\,0\,\lambda}(R_{\alpha L})}{\partial R_{\alpha L}} P_\lambda(\cos\psi_2)\sin\psi_2 + \sum_{\lambda\geq 2} \frac{V^{\,0\,0\,0}_{\lambda\,0\,\lambda}(R_{\alpha L})}{R_{\alpha L}} P^1_\lambda(\cos\psi_2)\cos\psi_2 \right). \quad (19)$$

The equations of motion of the three nuclei are:

$$\begin{aligned} M_L \ddot{\boldsymbol{r}}_L &= \boldsymbol{F}_{LH} - \boldsymbol{F}_{L\alpha} \\ M_H \ddot{\boldsymbol{r}}_H &= -\boldsymbol{F}_{LH} - \boldsymbol{F}_{H\alpha} \\ m_\alpha \ddot{\boldsymbol{r}}_\alpha &= \boldsymbol{F}_{L\alpha} + \boldsymbol{F}_{H\alpha}\,. \end{aligned} \quad (20)$$

Here we assumed that the two heavy fragments have the same multipolarity in deformations. In this paper we consider only quadrupole deformations.

The above system was solved numerically employing the `lsoda` package for ordinary differential equations, with automatic method switching for stiff and nonstiff problems [18].

In Figure 5 a, b, c we presented the trajectory of the three fragments for the two extreme initial conditions (with high and with low kinetic energies of the heavier fragments) in a sequence of 10 time steps. The time scale is divided into increments of $\Delta t = 1.8\times 10^{-22}$. In figure 5a we display the trajectories of one of the most asymmetric splittings, recorded in experiment, i.e. ^{152}Nd + ^{92}Kr. Since in this case the α feels a stronger repulsion from the heavy fragment, it will be deflected at a larger angle in the direction of the light fragment. In the case of the splittting ^{144}Xe + ^{104}Nd this deflection will be less pronounced (Fig.5b) and for the more equilibrated

splitting, i.e. ^{132}Nd + ^{116}Pd, the α will be only slightly deflected (Figure 5c). We thus observe that in all the cases the α-particle is deflected in the direction of the light fragment, but with a larger angle when the initial kinetic energy of the heavier fragments is higher. This fact should be attributed to the low energy of the α ($\leq$ 1MeV) which makes it to feel for a longer time the repulsion coming from the heavy fragment. In Table I we present the final kinetic energy E^f_α and the asymptotic angle θ^f_α for the three splittings mentioned above when we employ point-like and size dependent forces. In all cases we observe the decreasing of E^f_α with increasing tip distance d. The mean of these two energies is not far from the value of $\langle E^f_\alpha \rangle$ = 16.0 $\pm$0.2 MeV which is the most probable α-particle energy predicted by the trajectory calculation for the *hot* fission. Thus, the phenomenon of α-particle energy *amplification* in the cold fission seems to follow the same pattern like in normal fission. This effect should be attributed solely to the predominant effect of the Coulomb field and less to deformation or finite size effects. It should also be remarked the near constancy of the final LCP kinetic energy for different mass splittings at the same tip distance, a fact already remarked long time ago in spontaneous fission [6]. In what concerns the angles at which α-particles are emitted their dependence on the mass splitting is obvious. Deviations from the axis perpendicular to the fission axis increase with the mass ratio. The difference observed between the two sets of data points to an important influence of the geometrical factors, which however does not alter the general trends of the process.

Naturally one might next ask if the experimental status of the problem allows the comparison with the results presented in this paper. Up to now there are no special data on cold fission available since from the expermental side it would mean to set a trigger on neutronless events, which is very difficult to attain in practice. There are available data on the alpha (and other particles) spectra, as a function

of the total excitation energy, reaching TXE = 10 MeV within the experimental accuracy performed by the Darmstadt group with the DIOGENES setup, and in a more recent work at the MPI Heidelberg [19]. These data does not contain special effects in the alpha spectra, when the cold fission regime is approached, except that the mean energy increases nearly linearly with decreasing TXE. This would mean that if the linear dependency would be extrapolated to TXE = 0 MeV, i.e. when the scission configuration tends to become compact, like in our model, the average kinetic energy of the α will approach the value 17.5 MeV [19,20]. According to the calculations presented in this work a range between 12 MeV to 20 MeV should be expected for the final kinetic energy if we consider that the α particle occupies the lowest states in the pocket formed from the interaction with the two heavier fragments. Therefore the experiment doesn't show a distinctive α kinetic energy distribution for cold fission, a fact which is in agreement with the calculations we presented in this paper. In order to establish more precisely $\langle E_\alpha \rangle$ we should carry out Monte-Carlo calculations. The fact that the experimental value is slightly higher than in hot fission (15.9 MeV) is a sign that the α is emitted earlier in cold fission, according to the uncertainty relation for energy $\Delta E \cdot \Delta t \approx \hbar$.

IV. FINAL REMARKS

We presented a receipt to determine the initial conditions for trajectory calculations in the ternary cold fission of ^{252}Cf. Compared to the case when the fragments are emitted with high excitation energy, the initial conditions are restricted to a narrower range of values as a consequence of the peculiarities of the process, mainly the compact shape of the fragments.

In our model the α-particle cannot be emitted at a tip distance larger than 8

fm, because as we showed for such a distance the α particle is no longer under the influence of the attractive nuclear forces, and on the other hand we disregard tip distances smaller than 6 fm because the LCP wavepacket filling the lowest state in the potential well has a small probability to tunnel through the thick transversal barrier.

The location of the LCP was fixed at the electro-nuclear saddle point, which is also model-dependent. Due to the finite size and the deformations of the fragments this location will be shifted with respect to the location of the electrostatic saddle point, and consequently the outcome of the trajectory calculation will be altered to a certain extent.

The initial kinetic energy of the LCP was considered to coincide with the lowest level occupied in a one-dimensional harmonic potential well oriented perpendicularly to the fission axis. This energy is decreasing with the tip distance.

As have been pointed by Halpern [6], there is no reason to believe that the third-particle ejection rates should be independent of the initial angular momentum. In our case the spin of the parent nucleus (^{252}Cf) being zero the angular momentum imparted to the fragments and their relative angular momentum is mainly due to the creation of a molecular configuration at the scission point [22]. In the model presented in this paper we didn't took into account the influence of collective molecular excitations, like bending or wriggling, nor the torques exerted between the fragments during the quasiclassical motion. The inclusions of these supplementary degrees of freedom could alter the initial configuration. This would be an interesting topic for a future investigation of the scission configuration in ternary cold fission. Moreover the evolution from scission to the release point of the LCP should be done in a dynamical way, i.e. writing equations of motion not only for the translational and rotational degrees of motion but also for the dynamical change of deformation,

because one might suppose that even if the *trinuclear* system is almost cold the small excitation energy present in the reaction will induce a β-polarization of the fragments [21].

V. ACKNOWLEDGEMENTS

I would like to express my gratitude to prof.Ter-Akopian and prof.F.Gönnenwein for fruitfull discussions and encouragements during the completion of this work and to M.Rizea and dr.F.Cârstoiu for their kindness in offering me some routines used in the calculations. The informations on the experimental status of the alpha accompanied cold ternary fission provided by Prof.Mutterer and Dr.Kopachi is acknowledged. I am also very indebted to prof.Halpern who carefully read the manuscript and expressed critical remarks.

TABLES

TABLE I. The tip distance d, the initial kinetic energy, E_α^0, the final kinetic energy E_α^f and the asymptotic angle θ_α^f of the α, with point-like and with finite size Coulomb forces

Splitting	$d(fm)$	E_α^0 (MeV)	E_α^f (MeV)	θ_α^f	E_α^f (MeV)	θ_α^f
			Point-like forces		Finite-size forces	
	6	2.71	20.10	80.83	21.36	77.86
^{92}Kr+^{156}Nd	7	1.72	15.84	78.77	16.91	75.70
	8	0.85	11.25	75.42	12.10	73.14
	6	2.68	19.87	85.03	20.96	83.29
^{104}Mo+^{144}Xe	7	1.70	15.57	83.77	16.44	82.08
	8	0.82	10.82	81.63	11.47	80.32
	6	2.85	20.29	88.17	20.86	86.99
^{116}Pd+^{132}Sn	7	1.84	15.86	87.69	16.31	86.27
	8	0.96	11.53	85.68	11.19	86.93

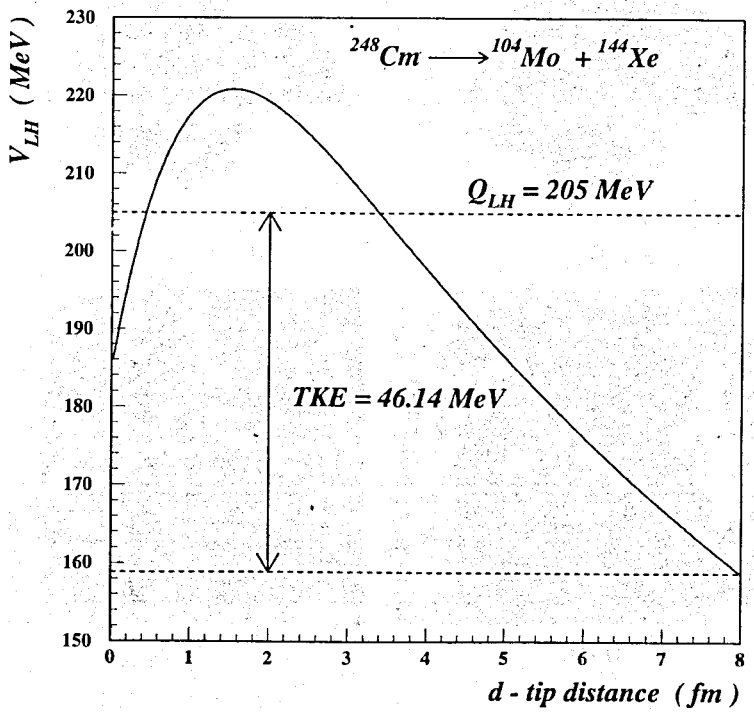

Fig. 1. The barrier between the two heavier fragments.

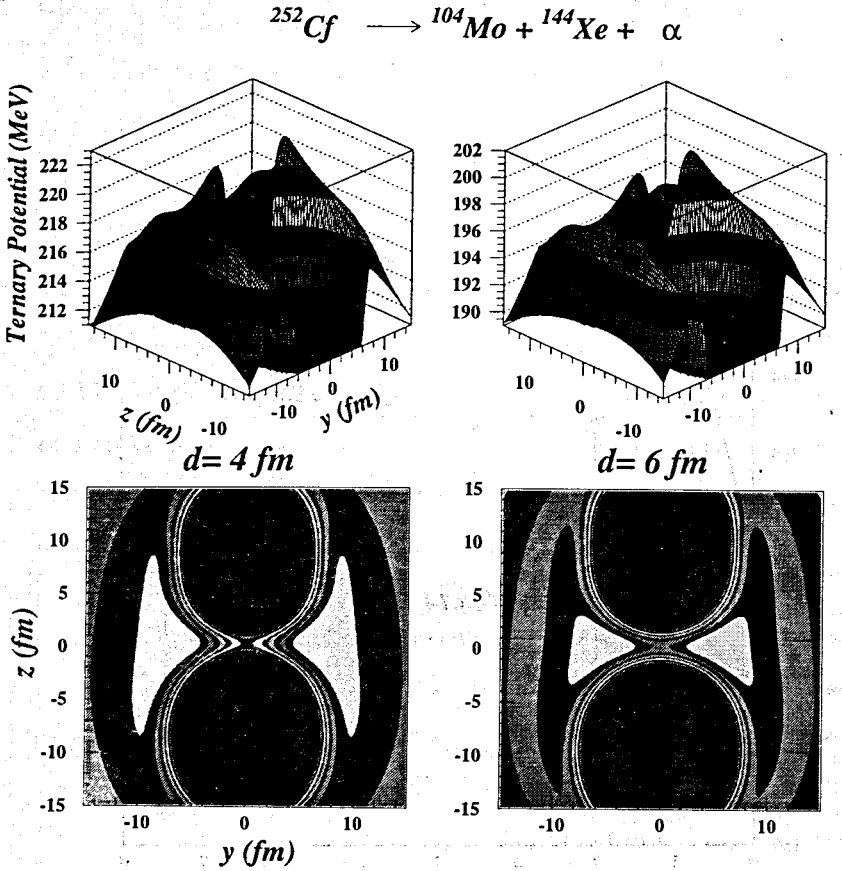

Fig. 2a. The barrier between the two heavier fragments for tip distances $d = 4$ fm and $d = 6$ fm.

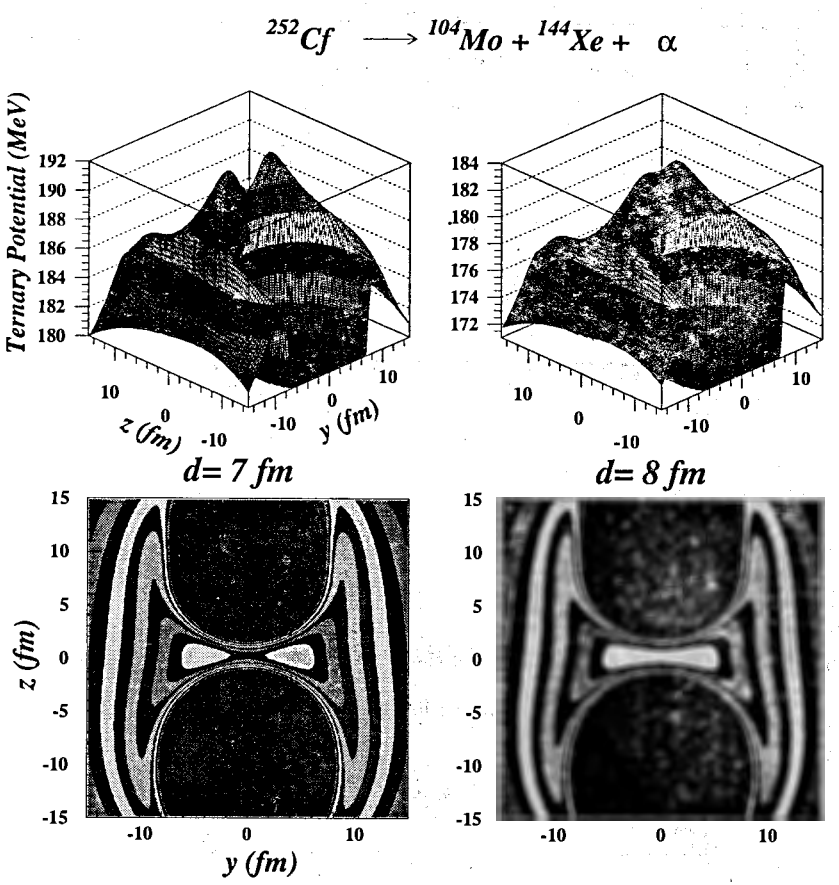

Fig. 2b. The barrier between the two heavier fragments for tip distances $d = 7$ fm and $d = 8$ fm.

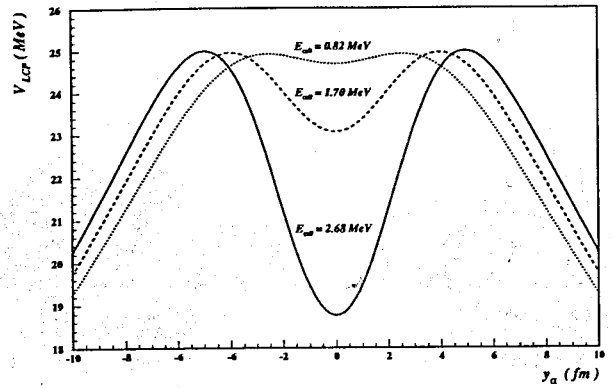

Fig. 3. The one-dimensional potential well of the α for three different tip distances : d = 6 fm (full line), d = 7 fm (dashed line), d = 8 fm (dotted line)

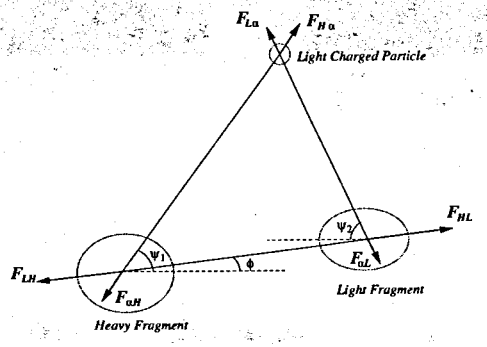

Fig. 4. The three-particle congfiguration and the forces acting between them.

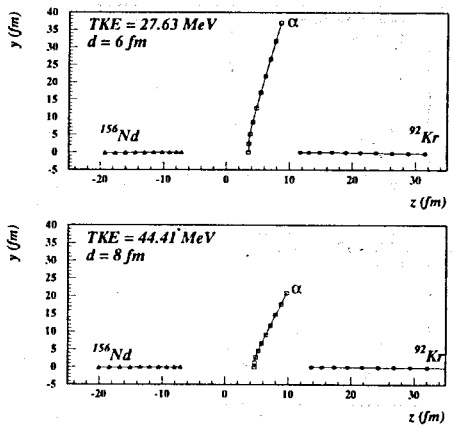

Fig. 5 a)

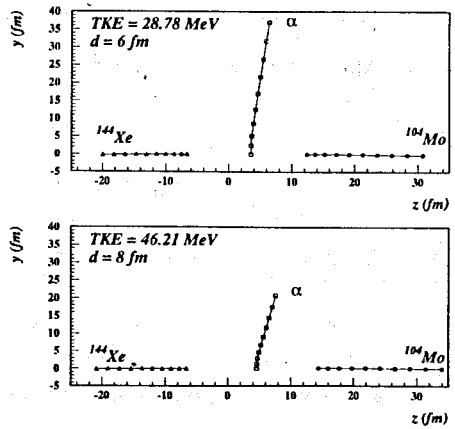

Fig. 5 b)

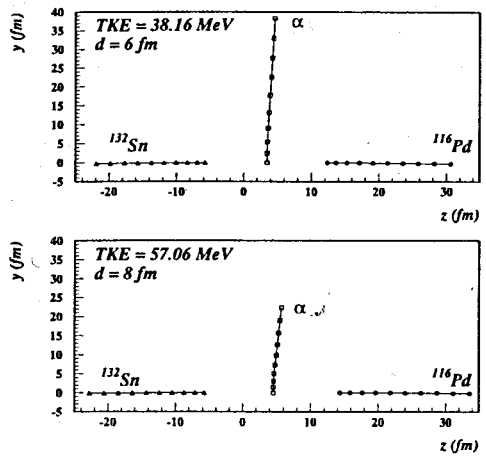

Fig. 5 c)

Fig. 5. The trajectory of the three fragments for the splitting a) ^{96}Kr + ^{152}Nd, b) ^{104}Mo + ^{144}Xe, c) ^{116}Pd + ^{132}Sn.

REFERENCES

[1] C.Wagemans, Ternary Fission, in: *The Nuclear Fission Process, Ed. C.Wagemans*, CRC Boca Raton FL, 1991

[2] F.Göennenwein et al., *6-th Int.Conf. on Nuclei Far from Stability and 9-th Int.Conf. on Atomic Masses and Fundamental Constants*, Bernkastel-Kue (1989) 453.

[3] A.V.Ramayya et al., *Phys.Rev. C* **57**, no.5 (1998).

[4] B.T.Geilikman and G.I.Hlebnikov, *At.Energya* **18** (1965) 218 (in russian).

[5] Y.Boneh, Z.Fraenkel and I.Nebenzahl, *Phys.Rev.* **156** (1967) 1305.

[6] I.Halpern, *Ann.Rev.Nucl.Sci.* **21** (1971) 245.

[7] P.Ertel, in P.Fong, *Statistical Theory of Nuclear Fission*, Gordon and Breach, Science Publishers, Inc., New York, 1969), p.191.

[8] P.Fong, *Phys.Rev.C* **2** (1970) 735.

[9] R.K.Choudhury and V.S.Ramamurthy, *Phys.Rev.C* **18** (1978) 2213.

[10] N.Cârjan and B.Leroux, *Phys.Rev.C* **22** (1980) 2008.

[11] H.Radi, J.O.Rasmussen, R.Donangelo, L.F.Canto and L.F.Oliveira, *Phys.Rev.C* **26** (1982) 2049.

[12] G.A.Pik-Pichak, *Yad.Fiz.* **40** (1984) 336 (in russian).

[13] K.T.R.Davies, A.J.Sierk and J.R.Nix, *Phys.Rev.C* **13** (1976) 2385.

[14] A.Săndulescu, F.Cârstoiu, Ş.Mişicu, A.Florescu, A.V.Ramayya, J.H.Hamilton

and W.Greiner, *J.Phys.G* **24** (1998) 181.

[15] A.Săndulescu, A.Florescu, F.Cârstoiu and W.Greiner, *J.Phys.G* **22** (1996) L87.

[16] F.Cârstoiu and R.J.Lombard, *Ann.Phys.N.Y.* **217** (1992) 279.

[17] A.Săndulescu, Ş.Mişicu, F.Cârstoiu, A.Florescu and W.Greiner, *Phys.Rev.C* **57**, no.5 (1998) 2321.

[18] L.R. Petzold, Siam J.Sci.Stat.Comput. **4** (1983) .

[19] M. Mutterer, *Private communication*, April 1998.

[20] Y. Kopachi, *Private communication*, April 1998.

[21] V. Avrigeanu, A. Florescu, A. Săndulescu and W. Greiner, Phys.Rev. C **52**, (1995) 1755.

[22] Ş.Mişicu, A.Săndulescu and W.Greiner, *Mod.Phys.Lett.A* **12**, (1997) 1343.

Received by Publishing Department
on May 12, 1998.